Nanoscale

Accepted Manuscript

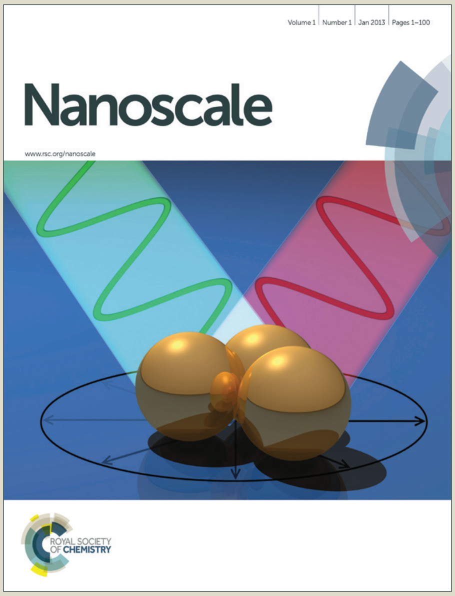

www.rsc.org/nanoscale

Journal Name

RSCPublishing

ARTICLE

Cite this: DOI: 10.1039/x0xx00000x

Received 00th January 2012,
Accepted 00th January 2012

DOI: 10.1039/x0xx00000x

www.rsc.org/

Nanocapsules Templated on Liquid Cores Stabilized by Graft Amphiphilic Polyelectrolytes

Joanna Szafraniec,[a] Małgorzata Janik,[a] Joanna Odrobińska,[a] and Szczepan Zapotoczny*[a]

A surfactant-free method of preparation of nanocapsules templated on liquid cores using amphiphilic graft polyelectrolytes was developed. A model photoactive copolymer, poly(sodium 2-acrylamido-2-methyl-1-propanesulfonate) with grafted poly(vinylnaphthalene) chains (PAMPS-*graft*-PVN) was used to stabilize toluene droplets in an aqueous emulsion. The macromolecules, due to their amphiphilic character and the presence of strong ionic groups, tend to undergo intramolecular aggregation in water but at the water-oil interface less compact conformation is preferred with PVN grafts anchoring in the oil phase and the charged PAMPS main chains residing in the aqueous phase thus stabilizing the nanoemulsion droplets. Formation of such nanocapsules was confirmed by dynamic light scattering measurements as well as SEM and cryo-TEM imaging. Grafting density and content of the chromophores in the graft copolymers were varied in order to achieve high stability of the coated nanodroplets. It was shown that the capsules are better stabilized by the copolymers with many short hydrophobic grafts than with fewer but longer ones. Use of photoactive polyelectrolytes enabled spectroscopic investigation of the relation between conformation of the macromolecules and stabilization of the oil-core nanocapsules. Long-term stability of the nanocapsules was achieved and further increased by multilayer shell formation using polyelectrolytes deposited via layer-by-layer approach. The obtained capsules served as efficient nanocontainers for a hydrophobic fluorescent probe. The proposed strategy of nanocapsule preparation may be easily extended to biologically relevant polymers and applied to fabricate liquid core nanodelivery systems without the need of using low molecular weight additives which may have adverse effects in numerous biomedical applications.

1. Introduction

The development of fabrication techniques of polymeric micro- and nanocarriers has attracted wide scientific interest in recent years.[1,2] Most of the works concerning controlled release strategies have been focused on increasing efficiency of encapsulation, improving protection of the encapsulated compounds and their prolonged release. Such structures are important in functional coatings for marine industry[3] and pharmaceutical applications requiring carriers for hydrophobic substances, e.g., lipophilic vitamins,[4] chemotherapeutic drugs,[5] hormones,[6] quantum dots[7] and magnetic particles.[8] Amphiphilic copolymers have been widely applied in the fabrication of nanocontainers and nanocarriers of hydrophobic drugs and other bioactive compounds. Such copolymers are believed to be better than low molecular weight surfactants for solubilization of sparingly water-soluble substances and stabilization of nanoscale delivery systems as, e.g., hydrogels[9] or micelles.[10] Although self-assembly of low molecular weight amphiphiles offers a possibility of preparation of the delivery systems, the thermodynamic instability of the formed structures is an issue. Typically millimolar values of critical micelle concentration (CMC) imply that a micellar system can dissociate into individual surfactant molecules upon dilution in the bloodstream with subsequent precipitation of the solubilized drug or other active agent. Hence, the alternative materials based on the amphiphilic polymers have been developed.[11-13] Polymeric micelles stabilized by block or graft copolymers with tailored architecture represent a class of efficient carriers, especially in terms of solubilization of hydrophobic compounds in polar media.[14] Although CMC values of the amphiphilic polymers are at the micromolar range, they may still disassemble upon dilution and/or due to increased ionic strength of fluids *in vivo*. To overcome this problem polymeric nanocapsules of core/shell structure were proposed.

Layer-by-layer (LbL) deposition method is one of the most commonly used techniques for the preparation of polymeric multilayer structures including capsules.[15,16] It is based on alternating adsorption of oppositely charged polyelectrolytes onto charged surface which leads to the formation of multilayer shells. For planar surfaces LbL is realized by consecutive immersion of a substrate in solutions of oppositely charged polyelectrolytes with intermediate step of rinsing the sample with pure water.[17] While considering formation of multilayer films on the dispersed micro- or nanoparticles it is important to avoid their aggregation prompted by the presence of the free polyelectrolyte and the applied separation procedure. The most commonly used techniques are centrifugation and membrane filtration that lead to efficient separation of the excess of polyelectrolyte solution from the coated particles but may also induce their aggregation, especially if the particles are soft and compliant (especially for coated liquid droplets). In the case of centrifugation an additional prerequisite is the density difference between the particles and the solvent. Saturation adsorption technique is advantageous when no separation of the particles from the solution is needed. In each deposition step the amount of added polyelectrolyte has to be carefully optimized in order to completely coat the surface of the particles but also to prevent flocculation which leads to formation of aggregates.[18]

The LbL technique was firstly introduced for preparation of multilayer shells on solid colloidal templates composed of polystyrene,[19] melamine formaldehyde,[20,21] calcium carbonate[22] or silica.[23,24] After removal of the template polymer capsules are formed with very thin shells (nanometers range) and aqueous cores. The formed multilayer shell enables its permeability to be tuned by varying its thickness and composition. Moreover, by the modification of the outermost layer of the shell it is possible to navigate the carrier and improve targeting of the encapsulated compounds.[25,26] However, low efficiency of encapsulation (especially hydrophobic compounds) and limited control of the capsule structure caused by incomplete etching of the core or damage of the shell during etching brought the need for other cores.

A feasible approach for encapsulation of the hydrophobic active molecules is using emulsion droplets as liquid templates instead of the solid cores.[27] Such a technique enables more effective encapsulation of hydrophobic molecules, however, the dynamic nature of the process of shell formation may be the limitation. The studies performed so far on the capsules with liquid cores stabilized by low molecular weight surfactants indicate that formation of a stable interfacial complex between surfactants and the first layer of polyelectrolyte plays a key role in formation of a stable shell of capsules.[28,29]

In this paper we present a novel way of stabilizing nanoemulsion droplets by amphiphilic graft polyelectrolyte poly(sodium 2-acrylamido-2-methyl-1-propanesulfonate)-*graft*-poly(vinylnaphthalene) (PAMPS-*graft*-PVN). In our previous work we presented the strategy of synthesis of graft amphiphilic polyelectrolytes with solvophilic backbone and solvophobic side chains.[30] Due to dual chemical nature, in polar media these macromolecules spontaneously aggregate forming hydrophobic domains consisting of packed VN grafts while at the water/oil interface the polymeric chains uncoil enabling stabilization of emulsion droplets by anchoring grafts without a need of using any additional surfactants. Such graft amphiphilic copolymers should ensure better stabilization of the oil nanodroplets than the block copolymers because in this case more hydrophobic graft per macromolecule anchor it at the water/oil interface.

It should be emphasized that the topology of macromolecular system strongly influences the conformations they adopt. Hence we have also studied here the influence of grafting density and content of the hydrophobic chromophores on the conformation of macromolecules and the related stability of the nanocapsules with liquid cores. Importantly, the synthesized copolymers play a double role in the system - they stabilize the emulsion droplets and act as the first layer of the capsule shell that was deposited using the LbL approach. Although the self-assembly process of the amphiphilic copolymers has been widely explored, especially for block copolymers, the reported structures include mainly micelles,[31] vesicles[32], and only rarely other structures[33], while capsules on liquid cores stabilized by graft amphiphilic polyelectrolytes with charged main chain have not been reported yet. Importantly, this novel surfactant-free method of stabilization of nanocapsules opens various opportunities for biomedical applications of such nanocapsules as drug delivery systems with large capacity for hydrophobic drugs, very good stability and additional LbL shells that may be tailored for required permeability and targeting.

2. Experimental

2.1. Materials

2-Vinylnaphthalene (VN, Aldrich, 95%) was purified by column chromatography using silica gel (pore size 60 Å, Fluka) as the stationary phase and cyclohexane (p.a., Avantor Performance Material Poland S.A.) as the eluent. 2-acrylamido-2-methyl-1-propanesulfonic acid (AMPS, 99%, Aldrich), 4-hydroxy-2,2,6,6-tetramethylpiperidinyl-1-oxyl (HTEMPO, free radical, 98%, Aldrich) 10-camphorsulfonic acid (CSA, anhydrous, 98%, Aldrich), poly(diallyldimethylammonium chloride) (PDADMAC, M_w<100000 g/mol, 35 wt.% in water, Aldrich), n-octadecane (p.a., Polyscience Corp.), polyethylenimine (PEI, Aldrich), iron(II) sulfate heptahydrate ($FeSO_4 \cdot 7H_2O$, ≥99.0%, Aldrich), hydrogen peroxide (30% solution, p.a., Avantor Performance Material Poland S.A., Poland), sodium hydroxide (NaOH, p.a., Avantor Performance Material Poland S.A.), sodium hydrogen sulfite ($NaHSO_3$, 40% wt.% in water, Avantor Performance Material Poland S.A.), potassium persulfate ($K_2S_2O_8$, p.a., Avantor Performance Material Poland S.A.), sodium carbonate (Na_2CO_3, p.a., Avantor Performance Material Poland S.A.), sodium chloride (NaCl, p.a., Lachner), dimethyl sulfoxide (DMSO, p.a., Aldrich), ethanol (96%, p.a., Avantor Performance Material Poland S.A., Poland), perylene (Pe, gold label, 99.9%, Aldrich), pyrene (98%, Aldrich) were used as received. Deionized water was used to prepare all the solutions.

2.2. Instruments and procedures

The UV-Vis spectra were obtained using Varian Cary 50 Conc spectrophotometer. ATR-FTIR spectra (on diamond) were collected using ALPHA FT-IR Spectrometer (Bruker). Elemental analysis was performed using Vario Micro Cube CHNS Analizer (Elementar). In order to prevent the formation of salts after combustion that could affect the results of elemental analysis the synthesized polymers, prior the analysis, were subjected to an ion-exchange procedure in order to remove sodium cations. Steady-state fluorescence spectra were measured at room temperature using an SLM Aminco 8100 spectrofluorimeter with a 450 W xenon lamp as a light source. Confocal microphotographs were collected using inverted microscope Nikon Ti-E with objective Plan Apo 100x/1.4 Oil DIC and confocal system Nikon A1. Dynamic (DLS) and static (SLS) light scattering measurements were performed using Malvern Zetasizer Nano ZS instrument working at 173° detection angle. The DLS measurements were performed at 22°C and the reported data represent averages (with standard deviations) of the mean hydrodynamic diameters determined from three series of measurements (10-100 runs each) applying distribution analysis algorithm (General Purpose mode) offered by the instrumental software. Field emission scanning electron microscope (FE-SEM, Hitachi S-4700) and transmission electron microscope (cryo-TEM, TECNAI F20 TWIN; staining with phosphotungstic acid) were used for imaging the nanocapsules. Viscosity was measured using Ubbelohde viscometer (SI Analytics, type 530 13/Ic) equipped with ViscoClock. The samples were freeze-dried using Christ Alpha 1-2 LD plus freeze dryer.

Scheme 1 Structure of the amphiphilic copolymer PAMPS-*graft*-PVN.

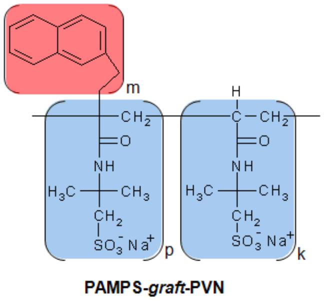

2.3. Polymer synthesis

PAMPS-*graft*-PVN (see Scheme 1) was synthesized via nitroxide-mediated free radical polymerization following general procedure described earlier[30] with some modifications. Briefly, the copolymer was obtained in three steps. First, the PAMPS homopolymer was synthesized. After neutralization of 5 g of AMPS with sodium carbonate, the solution was mixed with 12 ml of DMSO and after heating the redox initiator ($K_2S_2O_8$:$NaHSO_3$, 1:1 molar ratio, 1 mol%) and HTEMPO were added. The reaction was carried out at 125°C for 7.5 hours under continuous bubbling with nitrogen. The original procedure of obtaining PAMPS was modified here by increasing the concentration of HTEMPO in the feed ratio to 2.5 mol% and changing the nonsolvent for precipitation to cold ethanol. The polymer was dried in vacuum oven, dissolved in water, dialyzed (Roth, cellulose tubing, cutoff 3500 $g \cdot mol^{-1}$) for a week and freeze-dried. The macroinitiators were obtained in the reaction of previously synthesized PAMPS with Fenton's reagent (a mixture of H_2O_2 and $FeSO_4$, 1:1 molar ratio). The syntheses were carried out in water for 3 hours at room temperature and after heating to 40°C the excess of H_2O_2 was removed. Different degrees of substitution (DS) of the polymers with HTEMPO were obtained by varying the amount of Fenton's reagent with respect to number of AMPS mers.[34] The product was then mixed with NaOH in order to remove iron cations and after filtration dialyzed against water for 5 days. To obtain the graft copolymers VN and HTEMPO-substituted PAMPS (c.a. 1.2:1 molar ratio) were dissolved in 15 ml of DMSO in the presence of 10-camphorsulfonic acid (CSA, 0.01 M) as a rate-accelerating additive.[35] The reactions were carried out at 130°C for predetermined periods of time under continuous bubbling with nitrogen. By extending the reaction time between the macroinitiator and 2-vinylnaphthalene polymers with different length of hydrophobic grafts were obtained (see Table 1).

2.4. Molar mass determination

SLS measurements were used for the determination of molar mass of PAMPS applying the measured refractive index increment (dn/dc= 0.143 ml/g). A number of the polymer solutions in 1 M NaCl with concentrations ranging from 1 to 4 g/L were measured and toluene sample was applied as a scattering standard. The Debye plot was used to calculate the molar mass of PAMPS. The viscosity average molar mass was calculated based on measurements of a series of PAMPS dilutions (from 0.02 mg/mL) and pure solvent (1 M NaCl) using an Ubbelohde viscometer.

2.5. Solubilization procedure

Fluorescent probes were solubilized in the aqueous solutions of the graft copolymers (c≈5 mg/mL) by slow injection of microliter volumes of the probe solutions (c≈10^{-4} M in methanol) into milliliter volumes of the polymer solutions. The solutions were vigorously stirred, purged with argon in order to remove the residues of methanol, and equilibrated in darkness for at least 2 hours before measurements.

2.6. Preparation of capsules on liquid cores

Polymeric capsules were obtained directly by mixing toluene and PAMPS-*graft*-PVN solution (1 g/L in 0.1 M NaCl) in 1:10 volume ratio. The mixture was sonicated for 30 minutes in an ultrasonic bath (540 W, Sonic-6, Polsonic) at room temperature. Multilayer shells were obtained via LbL saturation method without intermediate rinsing with water during continuous mixing with a magnetic stirrer at 450 rpm (see Figure 1). Volumes of the polyelectrolyte solutions (PAMPS and PDADMAC respectively, c=1 g/L in 0.015 M NaCl) for each layer were optimized based on the simultaneous zeta potential and particle size distribution measurements.

2.7. Preparation of capsules for SEM imaging

The capsules for SEM measurements were prepared by emulsification of PAMPS-*graft*-PVN (1 g/L in 0.1 M NaCl) with n-octadecane (100:1 volume ratio) in ultrasonic bath at 32°C. After 30 minutes of sonication the obtained capsules on liquid n-octadecane cores were cooled down to room temperature which caused solidification of n-octadecane. The obtained nanocapsules were then deposited on a silicon wafer by placing a droplet of the emulsion on the surface that was previously cleaned with "piranha" solution (a mixture of H_2SO_4 (96%) and H_2O_2 (30%), 1:1 volume ratio) and coated with a cationic polyelectrolyte (by immersion in PEI solution (1 g/L) and sonication for 5 min) for stronger interactions with negatively charged capsules. Then, the surface was carefully rinsed with water and dried in a stream of argon.

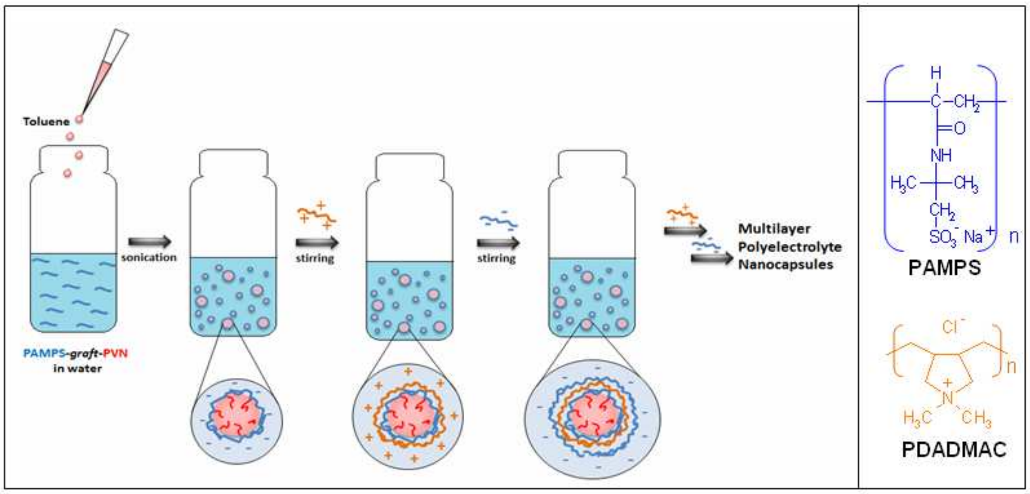

Figure 1 Scheme of preparation of multilayer nanocapsules on liquid core stabilized by PAMPS-*graft*-PVN.

2.8. Encapsulation studies

Perylene was used as a fluorescent molecular probe for encapsulation studies. The microliter volume of probe solution in methanol was added to mixture of copolymer solution and toluene and sonicated for 30 minutes at room temperature. The concentration of the probe in the capsules was ca. 10^{-5}M.

3. Results and discussion

3.1. Characterization of the synthesized polymers

The precursor PAMPS homopolymer was synthesized and characterized. The viscosity average molecular weight calculated using Mark-Houwink equation was found to be equal to 36000 g/mol,[36] and the weight average molecular weight from the static light scattering measurements was determined to be 51000 g/mol, similarly to the previously reported values.[30]

In the second synthetic step PAMPS was functionalized with HTEMPO groups that were attached along the chains leading to PAMPS-*graft*-HTEMPO. The degree of substitution (DS) of PAMPS with HTEMPO (grafting density) was determined via elemental analysis (Table 1). DS increases with increasing the Fenton's reagent : PAMPS ratio. However, this relation was not linear which may be caused by oxygen species present in the reaction mixture decreasing the amount of free radicals and varying efficiency of detachment of hydrogen atoms from the polymer chain. Finally, PAMPS-*graft*-HTEMPO polymers were used as macroinitiators for polymerization with VN leading to PAMPS-*graft*-PVN copolymers. The composition of the graft copolymers could not be calculated based on elemental analyses due to very scattered data that generally underestimated the content of nitrogen. The content o naphthalene chromophores in the graft copolymers was finally determined based on the IR spectra of the copolymers using appropriate calibration.[30] Briefly, IR spectra of a series of blends containing PAMPS and VN mixed at different weight ratios and those of PAMPS-*graft*-PVN copolymers were collected and the intensity of the band between 874.3 cm^{-1} and 912.3 cm^{-1}, which was assigned to C-H bending in the naphthalene ring, was calculated for each sample. The IR spectra for the selected system and the assignment of vibrations characteristic of aromatic groups for the whole series of copolymers are available in Supporting Information (Figure S1 and Table S1). The length of hydrophobic grafts generally increased with prolonging the polymerization time, however the growth was fastest during the first three hours of the reaction. For syntheses lasting 6 hours or longer only slight changes in the amount of grafted VN were observed. Most likely, the prolonged heating of the reaction mixture leads to the reduction of the number of active graft ends lowering the overall polymerization yield. Unfortunately, the content of the chromophores grafted onto PAMPS chain could not be determined based on 1H-NMR spectra as the mobility of bulky aromatic group in the confined environment is restricted.[37]

3.2. Conformation of the graft copolymers – DLS studies

Conformation of the polymeric chains was studied using dynamic light scattering measurements which enable determination of the hydrodynamic size of the objects in solutions. The measurements performed in water show different behavior of the chains depending on the grafting density and the content of VN units (see Table 2 and Figure S2 in SI). The investigated systems, except for G1-3h, adopt very compact conformation with diameter between 5.2 and 8.3 nm which may be assigned to the formation of highly-packed intermolecular aggregates. (note that for the PAMPS homopolymer the hydrodynamic diameter was found to be 3.8±0.1 nm). This is in accordance with the fluorescence probe studies (see further) that also indicated that the copolymers with higher content of VN units form packed structures.

G1-3h copolymer forms more spacious structures with average diameter equal to 69.3±0.8 nm which confirms that the graft copolymer with low enough content of chromophores arranged in short grafts is able to form intermolecular aggregates in water. Similar situation was observed for the copolymer of poly(vinylnaphthalene) grafted onto poly(vinyl alcohol) (PVA-*graft*-PVN) which also aggregated in polar media forming structures of average diameter equal to 255 nm. Charged PAMPS-*graft*-PVN copolymers due to repulsive interactions between the chains seem to have lower tendency for the formation of intermolecular aggregates than uncharged PVA-*graft*-PVN. However, after prolonged storage (3 month) some aggregates with average size of 20-90 nm also appeared in the PAMPS-*graft*-PVN aqueous solution indicating dynamic behavior and rearrangement of such macromolecules in water. What is more, dissolution of the copolymers in DMSO causes relaxation of the structure and partial uncoiling of the polymeric chains that promotes to some extent intermolecular aggregations. PAMPS-*graft*-PVN with the lowest grafting density and shortest PVN grafts forms structure with diameter of about 50 nm, while other systems tend to form intermolecular aggregates of diameter between 200 and 370 nm as measured by DLS.

Table 1 Molar ratios of reagents used in the syntheses and compositions of the resulting polymers.

Sample/ polymerization time		AMPS mer : Fenton's reagent	Grafting density[a] [%]	Content of VN [b,c] [wt %]	Average number of VN per graft
G1	3h	1 : 0.03	1.2±0.03 (2.1 per chain)[d]	5.2±1.0	3.3
	6h			5.6±1.1	3.5
	9h			6.8±1.4	4.2
G2	3h	1 : 0.15	2.1±0.3 (3.7 per chain)[d]	9.7±1.9	3.4
G3	3h	1 : 0.3	9.9±2.3 (17.5 per chain)[d]	6.5±1.3	0.5

[a] determined via elemental analysis (C, N content in the polymer);
[b] determined by calibration based on IR spectra;
[c] error was estimated to be 20% of the calculated value;
[d] calculated taking into account the viscosity average molecular weight of 36000 g/mol.

Table 1~~2~~ Average particle size by volume obtained via DLS measurements of the copolymer aqueous solutions.

Sample	Diameter (nm)
G1-3h	69.3±0.8
G1-6h	5.2±0.5
G1-9h	5.4±0.3
G2-3h	7.1±1.0
G3-3h	8.3±0.7

3.3. Spectroscopic studies of the graft copolymers

UV-Vis spectroscopy. Conformations of the copolymer chains were further investigated spectroscopically. The UV-Vis absorption spectra of the graft copolymers showed flattened, tailed band extended even up to ca. 500 nm for G1-3h (see Figure 2). Such flattening of the structured band at ca. 290 nm, characteristic of the naphthalene chromophore, confirms the aggregation in the aqueous solutions of the copolymers, as it was previously found experimentally[30,34] and described theoretically.[38] Interestingly, the greatest batochromic extension of the band was observed for G1-3h copolymer that has the lowest content of the naphthalene chromophores. It may be explained in terms of the postulated intermolecular aggregation of partially uncoiled chains that leads to the formation of larger clusters that also absorb at longer wavelengths.

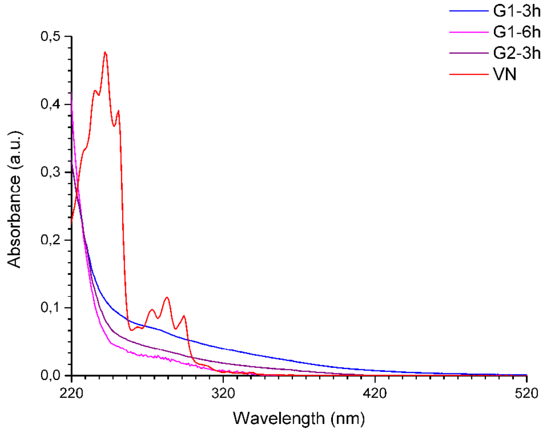

Figure 1~~2~~ UV-Vis absorption spectra of PAMPS-*graft*-PVN in the aqueous solution (c= 0.1 g/L for all the polymers) and of VN in methanol.

Fluorescence studies. As the interactions between naphthalene chromophores influence their photophysical properties, fluorescence spectra were collected to determine conformations of the polymeric chains.[38] Also in these studies G1-3h showed different spectral characteristics as compared to other copolymers. One can notice that the emission of G1-3h appeared not only when the excitation wavelength applied was 280 nm (as for isolated VN chromophores) but even for 420 nm. The latter emission could be assigned to the formed naphthalene aggregates (see Figure 3). Moreover, the long-wavelength fluorescence intensity decreases in DMSO which is a non-selective solvent and encourages uncoiling of the polymeric chains and partial disintegration of the formed intermolecular aggregates. The fluorescence excitation spectra also confirm the formation of intermolecular aggregates in water that absorb at much longer wavelength than isolated naphthalene chromophores (compare the absorption spectrum of VN in Figure 2 and the excitation spectra in Figure 3). Such aggregates do not seem to be completely disintegrated in DMSO where fluorescence can be recorded for excitation wavelengths up to ca. 410 nm (see Figure 3 lower panel).

In our previous work we postulated so-called “pearl necklace” conformation for PAMPS-*graft*-PVN chains in an aqueous solution.[30] As the lengths of the hydrophobic grafts of that copolymer and presented here G1 and G2 systems are comparable one can expect formation of “pearl necklace” conformation of those polymers. In fact, for the copolymers containing longer or more densely grafted VN chains compared to G1-3h the proposed “pearl necklace” conformation seems to be valid. Even the long-wavelength emission is much less pronounced for those copolymers (see Figure 4 for G1-6h and Figure S4 in SI for other polymers). It may be explained by the formation of highly packed intermolecular aggregates within the separated “pearls” formed along the chains. Thus, in addition to residual monomeric fluorescence (below ca. 360 nm) only the fluorescence of aggregates may be observed with such low intensity that Raman scattering signals (indicated with stars in Figures 3, 4, and S3 in SI) of water molecules contribute significantly or dominate the spectra. In DMSO, slightly more intense emission at longer excitation wavelength was observed for the studied copolymers indicating some loosing of the “pearls” but not complete uncoiling of the chains.

Interestingly, the conformation of PAMPS-*graft*-PVN chains seem to be very sensitive to the content of VN mers as G1-3h and G1-6h do not differ much in composition but their tendency to undergo inter- or intramolecular aggregation in water is different. It seems also that both the length of vinylnaphthalene grafts and the grafting density play an important role in the conformation the macromolecules even for similar overall composition. While G1-9h and G3-3h have similar VN content, due to the difference in their molecular architecture their hydrodynamic diameters differ noticeably, what strongly influences the ability of the copolymers to stabilize the formed nanocapsules (see below).

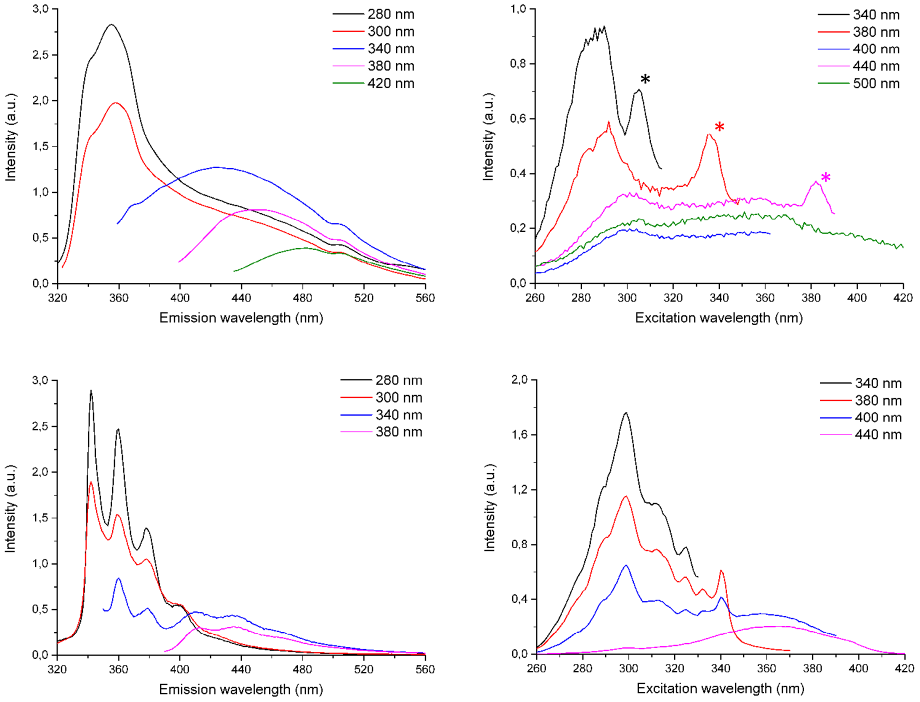

Figure 2~~3~~ Steady-state fluorescence emission (left panel) and excitation (right panel) spectra of PAMPS-*graft*-PVN (G1-3h) dissolved in water (upper) and DMSO (lower).

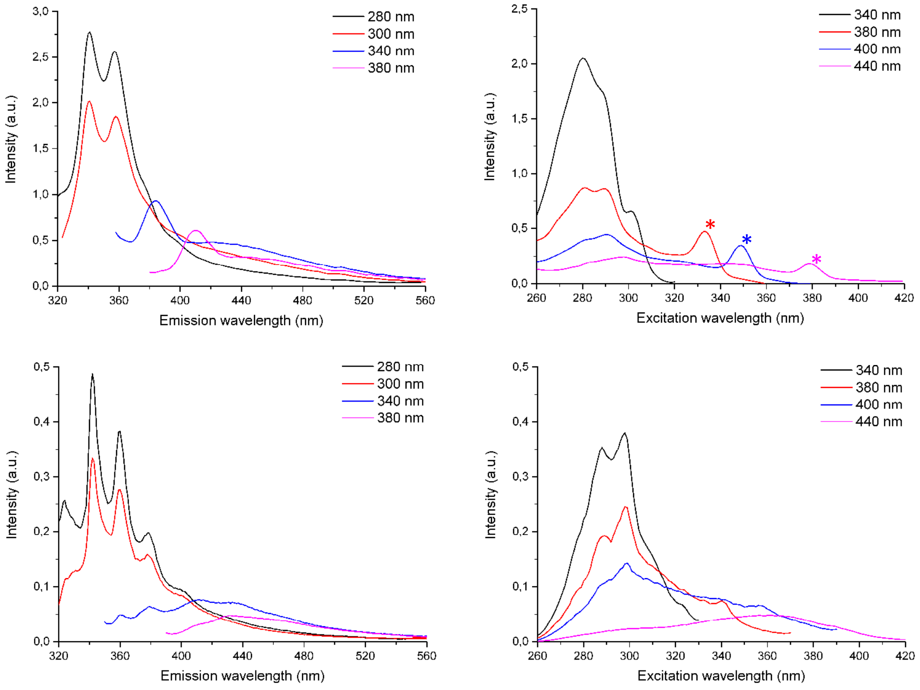

Figure 4 Steady-state fluorescence emission (left panel) and excitation (right panel) spectra of PAMPS-*graft*-PVN (G1-6h) dissolved in water (upper) and DMSO (lower).

Fluorescence probes studies. Pyrene was used as an indicator of the polarity of the polymer phase in aqueous solution as the intensity of the vibronic fine structure of the monomeric form of pyrene depends on the polarity of the environment.[39] The ratio of the emission intensities of peak III (at ca. 382 nm) and peak I (at ca. 372 nm) varies with changes in the grafting density and content of hydrophobic chains (see Table 3 and Figure S5 in SI). The values are in the range of those measured for water and ethanol suggesting that pyrene is located in the environment strongly penetrated by water molecules - rather in the interfacial area than in the interior of the hydrophobic polymer domains. It is particularly noticeable for the G1-3h system, for which the I_{III}/I_I ratio is the lowest (0.50), as its relatively spacious intermolecular aggregates are easily penetrated by water molecules. For the copolymers containing more VN units the value of I_{III}/I_I ratio increases only slightly. Nevertheless, the obtained results indicate that the inner parts of the cramped polymeric pearls are hardly available for pyrene molecules due to high packing of those domains in the aqueous medium.

Table 2~~3~~ Ratios of emission intensities of peak III (at 382 nm) and peak I (at 372 nm) of pyrene solubilized in the aqueous solutions of the graft copolymers.

Sample	I_{III}/I_I
G1-3h	0.50
G1-6h	0.57
G1-9h	0.60
G2-3h	0.53
G3-3h	0.55
Water	0.49
Ethyl alcohol	0.62

Therefore, perylene was used as another probe to study the formation of hydrophobic domains in the aqueous solution of the copolymers as its fluorescence appears only in non-polar environment.[40] The weak fluorescence of perylene solubilized in G1-3h solution is a result of ineffective solubilization of the probe in loosely packed intermolecular aggregates (see Figure 5). With increasing the content of VN the signal increases significantly (see Figure 5 for G1-6h) as the probe has a stronger tendency to enter well-defined hydrophobic domains. Qualitatively similar results were obtained for the remaining copolymers with postulated pearl-necklace conformation.

Microviscosity of the polymeric hydrophobic domains was checked by measuring the fluorescence polarization of the solubilized perylene.[41] The values of the fluorescence anisotropy (r) obtained for the copolymers varied between 0.2 and 0.35. It confirms that perylene molecules, if solubilized, are located in highly packed polymeric domains as the probes experience highly viscous environment similar to that of glycerol (r=0.33±0.01).[42] These values are also similar to the values obtained previously for block amphiphilic copolymers containing VN mers.[43]

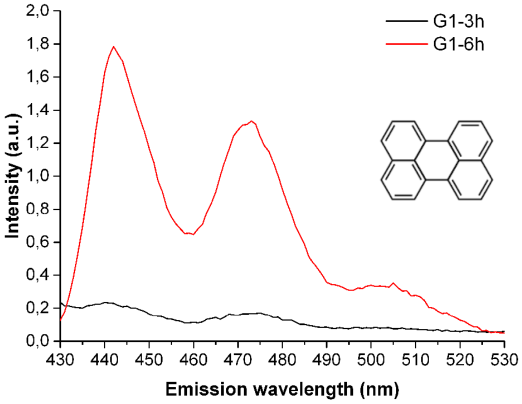

Figure 5 Steady-state fluorescence emission spectra of perylene solubilized in the aqueous solutions of G1-3h and G1-6h (c≈5 g/L, λ_{ex}=410 nm).

3.4. Nanocapsules fabricated on liquid cores

Preparation of nanocapsules. The polymeric nanocapsules templated mainly on toluene liquid cores were prepared by simple mixing of the non-polar solvent with the aqueous solution of PAMPS-*graft*-PVN copolymers serving as stabilizing agents. Different fabrication conditions were tested in order to optimize the formation of the capsules mainly with respect to their size and long term stability. We found that not only the composition of the used copolymers, but also the type of solvent, order of mixing, and the ratio of reagents play important roles in the effective stabilization of the obtained structures.

Formation of the nanocapsules was followed using electron microscopies (see Figure 6 and 7 for G3-3h system) and DLS measurements (Figure 8). The G3-3h system was selected for those studies as it forms the most stable nanocapsules (see below). For the SEM measurements the nanocapsules were formed at elevated temperature (32°C) on liquid n-octadecane cores that solidify upon cooling below the melting temperature (26-28°C). Such nanocapsules could be easily manipulated and did not disintegrate under vacuum during SEM imaging. Moreover, changing the hydrophobic core did not significantly affect the properties of the capsules. The performed DLS measurements confirmed that in both experimental series we obtained the capsules of similar properties – average hydrodynamic diameters equal to 147±10 nm and 123±2 nm, and zeta potential -37±4 mV and -30±3 mV for the capsules on toluene and n-octadecane cores, respectively, were measured.

Spherical objects were clearly observed in SEM images and cryo-TEM images confirming formation of spherical capsules of diameters between ca. 50-300 nm (see Figure 7). The observed relatively broad size distribution of the nanocapsules may be a result of different morphology of macromolecules that stabilized the capsules as grafting density and length of hydrophobic grafts of the stabilizing macromolecules likely varied in the samples. Although the size distribution is rather broad the process of aggregation of the capsules was almost completely inhibited what is crucial concerning their further applications as eg. nanocarriers. Several shapeless structures visible at the captured micrographs were assigned to fragments of macromolecules that were not involved in the process of stabilization of the emulsion.

DLS measurements of the same capsules (stabilized by G3-3h) revealed similar average hydrodynamic diameters that also slightly varied with time (see Figure 8). The average hydrodynamic diameters of the nanostructures stabilized by the other copolymers vary in the range of ca. 30–150 nm (see Figure 8). It should be noted that the DLS results revealed rather broad size distribution (polydispersity index, PDI, values in the range of 0.36-0.52) that might not reflect the actual sizes of the cores due to contribution of the chains loosely connected with the surface of the capsules, or aggregates of nanocapsules (overestimated sizes), and free macromolecules present in the emulsion (underestimated sizes) (see Figure S7). Such broad and sometimes multimodal distributions may be also partially explained by the lack of filtration, which is commonly applied before DLS measurements. In the case of nanocapsules such a treatment might have destroyed some of them so we omitted this step.

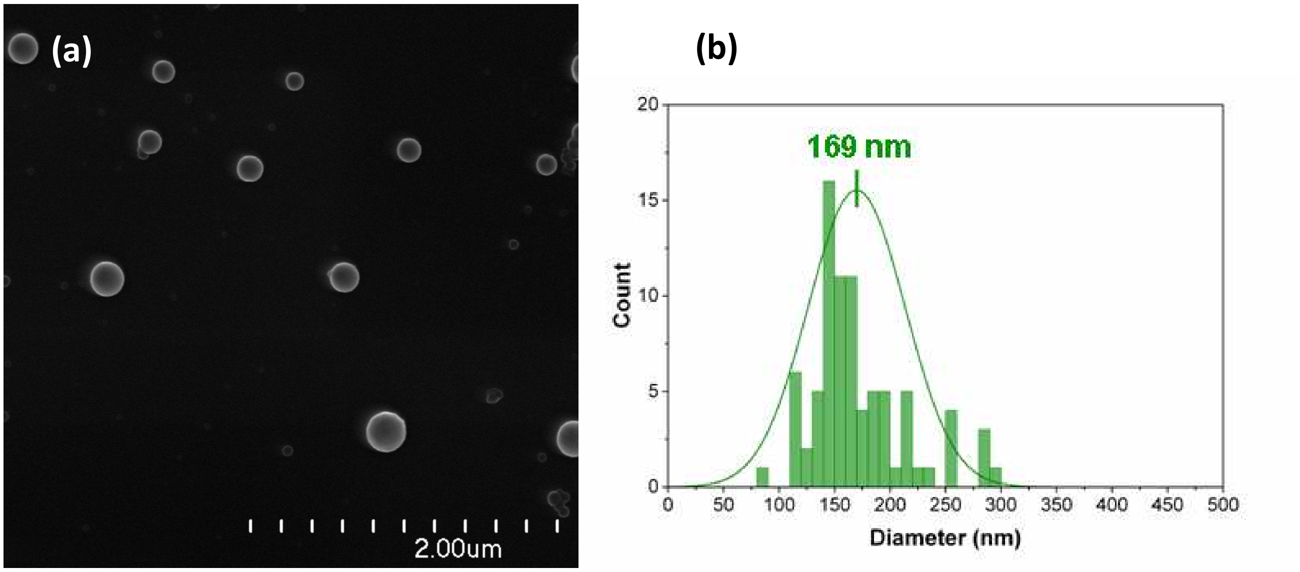

Figure 6 SEM image of G3-3h capsules template on n-octadecane cores (a) and a histogram of their size distribution (b).

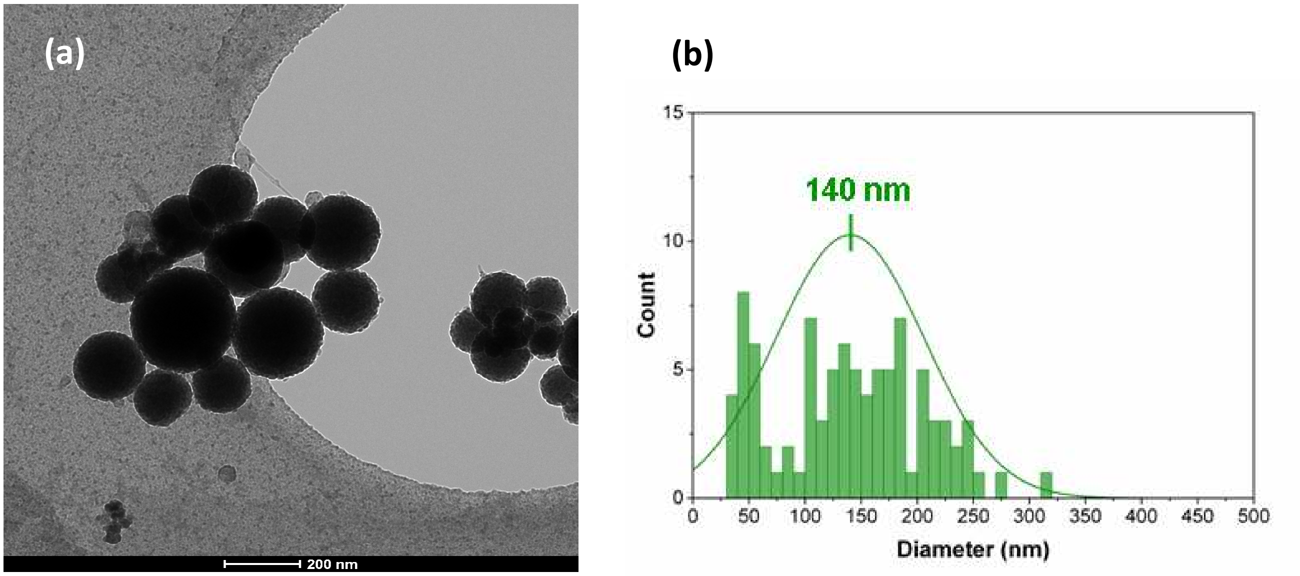

Figure 7 Cryo-TEM image of the stained capsules stabilized by G3-3h obtained on toluene core (a) and a histogram of their size distribution (b).

Nevertheless, high absolute values of zeta potential (ζ) measured for the capsules immediately after sonication (Figure 8 and Table S3) indicated also high potential of the graft amphiphilic polyelectrolytes for preparation of stable capsules with liquid cores. Importantly, certain relationships between the size and zeta potential of the nanocapsules, on one side, and the architecture and composition of the applied copolymers, on the other, may be observed. For G1-3h system the value of zeta potential just after the preparation (-8.8 mV) did not satisfy the common stability criterion of colloidal systems ($\zeta > |30|$ mV) due to insufficient number of hydrophobic grafts which are necessary to anchor the polymer in the non-polar core and bring the negative charge of PAMPS chains to the water-oil interface. Moreover, two months after preparation of the capsules the PDI reached the value of 0.89 suggesting very low stability of the dispersion making DLS results unreliable (they were not included in Figure 8). Increasing the length of the grafts while keeping the same grafting density (G1-6h and G1-9h systems) improves stability of the formed nanocapsules as indicated by more negative zeta potential values. This observation is important as one might expect that the copolymers having more compact conformations compared to G1-3h should be less likely to uncoil at the water-oil interface. However, even for those systems after two months of storage at room temperature only small objects were observed by DLS (ca. 7 nm and 10 nm for G1-6h and G1-9h, respectively) with sizes comparable to the hydrodynamic diameters of the applied copolymers (see Table 2). It seems that even longer grafts do not stably anchor at the interface and the copolymers are transferred to the aqueous phase leaving unprotected oil droplets that coalesce. Nevertheless, increasing the grafting density in the studied copolymers seems to significantly improve the stability of the oil droplets. High values of the zeta potential (reaching ca. -37 mV) over time up to two months of storage confirmed long-term stability of the nanoemulsions stabilized by G2-3h and G3-3h copolymers. Moreover, the capsules stabilized by G2 and G3 copolymers do not change noticeably their sizes in time.

Fluorescence studies were also used to investigate the ability of the macromolecules to uncoil at the water/oil interface as a prerequisite for efficient anchoring of the copolymer at the water-oil interface (Figure 9). It is expected that the formed molecular aggregates become less packed (due to partial uncoiling of the chains) when hydrophobic grafts are involved in the stabilization of the emulsion droplets. In fact, the emission spectra of the capsules stabilized by G1-3h have different shape with much smaller contribution of aggregates compared to the copolymer spectra in water. In particular, large aggregates seem to completely disappear in the capsules as the emission intensity for the excitation wavelength of 400 nm is close to zero. Similarly, for G3-3h (Figure 9) and other copolymers the intensity of long-wavelength emission follows the same trend confirming (partial) uncoiling of the "pearls" and anchoring of VN grafts in the oil droplets.

Figure 8 Hydrodynamic diameters by number and zeta potential of capsules stabilized by a series of PAMPS-*graft*-PVN copolymers at different time after preparation (day 0, 7, 17 and 60, respectively). Error bars represent standard deviations of the measured values. Red star in the first graph indicates unreliable data due to very broad size distribution.

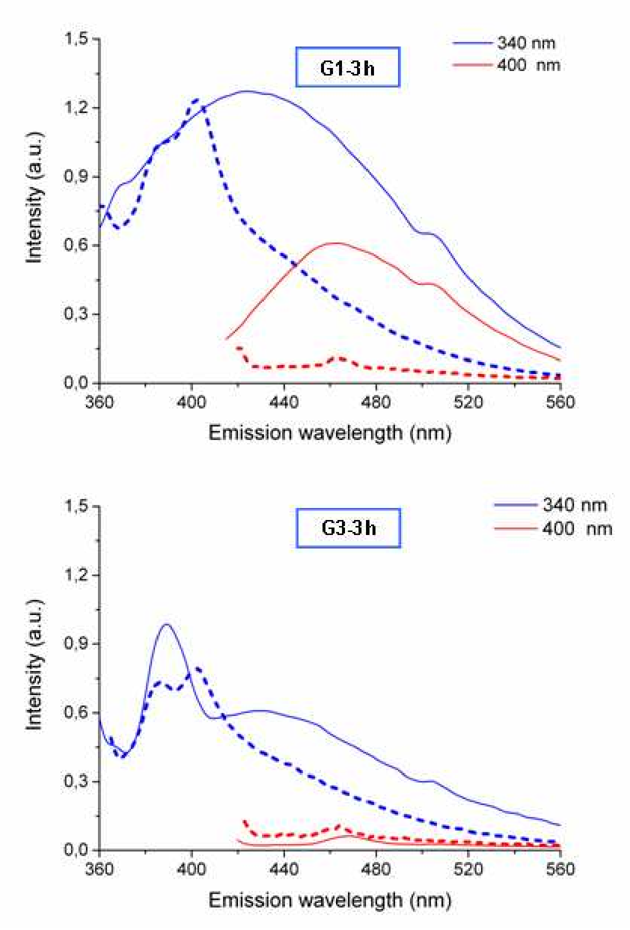

Figure 9 Steady-state fluorescence emission spectra of PAMPS-*graft*-PVN (solid lines) and capsules (dotted lines) stabilized by G1-3h system (upper) and G3-3h (lower) upon excitation at wavelength (given in the legend) absorbed by molecular aggregates of VN.

Nanocapsules coated with multilayer shells. The multilayer polyelectrolyte shells was formed via LbL adsorption of PDADMAC and PAMPS polyelectrolytes onto oil cores stabilized by PAMPS-*graft*-PVN. Zeta potential measurements were used to control the process of adsorption of each layer. Exemplary plot of zeta potential (Figure 10a) is of the typical zigzag shape which confirms alternating adsorption of the polyelectrolytes and strong electrostatic stabilization of the capsules. Interestingly, the measured values confirm that for all the studied systems stable nanocapsule dispersions were obtained. All the results of the zeta potential measurements presented in Table S3 in SI show that the stability of the emulsion increases after coating capsules with polyelectrolyte shells for the copolymers of all series. However, as it may be expected from the lowest content of VN mers for the G1-3h system the values of zeta potential of the capsules stabilized by this copolymer indicate their lowest stability. For all the systems but G1-3h, the values of zeta potential after deposition of forth layer are lower than -30mV and the adsorption of each new layer causes further increase of the absolute value of zeta potential. Formation of each layer of the shell was also confirmed by the measurements of the size of the coated capsules. Their average hydrodynamic diameter increased gradually with deposition of each next layer (Figure 10b) which confirms alternating adsorption of the oppositely charged polyelectrolytes without undesired aggregation of the coated capsules.

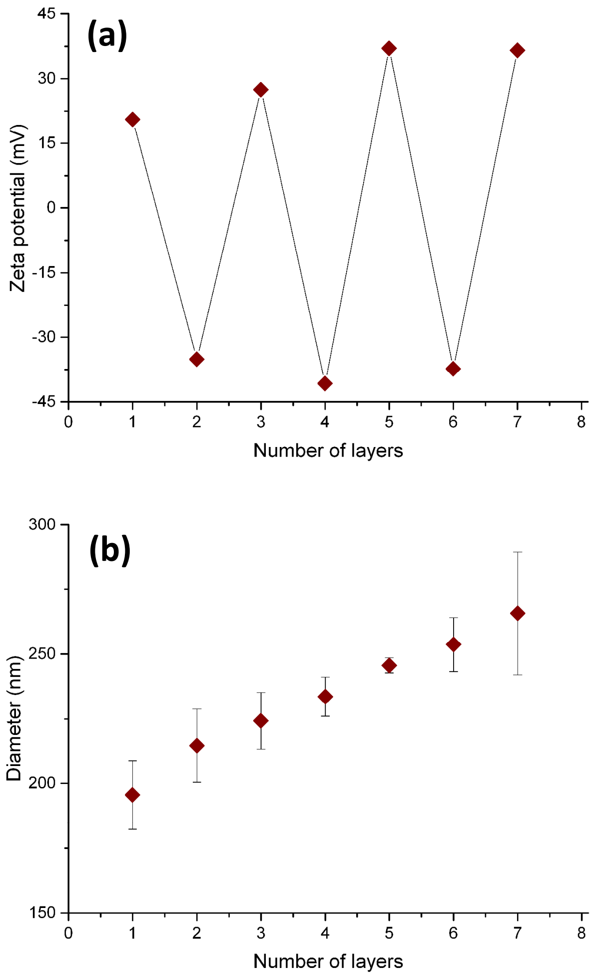

Figure 10 Zeta potential (a) and size by volume (b) of capsules stabilized by copolymer G3-3h as a function of number of PDADMAC and PAMPS polyelectrolyte layers.

Encapsulation of molecular probes into the nanocapsule cores. The possibility to encapsulate hydrophobic compounds inside the oil cores was confirmed using perylene as a fluorescent probe. The DLS studies showed that no deviations from regular growth of the shell size were observed for the loaded capsules as compared to the unloaded ones (see Figure S6 in SI). It suggests that the probe molecules are situated inside the core rather than incorporated into the shells. Moreover, the size PDI values for the loaded nanocapsules vary in the range of 0.2 to 0.4 indicating their more homogeneous size than observed for the unloaded ones (PDI in the range 0.2-0.8). The encapsulated perylene molecules retain their ability to fluoresce as confirmed by measurements of the fluorescence emission spectra and confocal microscopy (see Figure 11). In the emission spectra one can observe the emission of perylene excited at 410 nm which confirms its presence in the hydrophobic core. There is also a very weak signal of perylene excited indirectly via energy transfer from naphthalene chromophores excited at 280 nm but the efficiency of this energy transfer is rather low. It is clear that only the perylene molecules located close to the shell containing naphthalene chromophores may be excited via energy transfer while majority of the perylene molecules present in the core are too far from the shell. Imaging with confocal microscopy confirms spherical shape of the capsules and a very small fraction of their aggregates. Those observations are very important for potential applications as they indicate that the prepared nanocapsules may be used as aggregation-resistant nanocontainers for hydrophobic compounds.

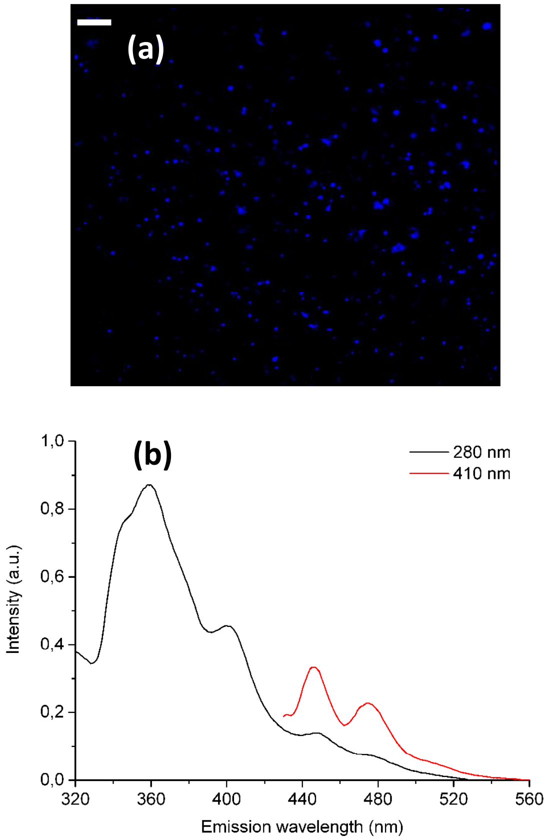

Figure 11. Confocal microphotograph (a) (scale bar: 10 µm, λ_{ex}=405 nm, DAPI filter) and (b) fluorescence emission spectra of the capsules with toluene cores stabilized by G3-3h and coated with 4 PDADMAC/PAMPS layers containing encapsulated perylene excited at 280 nm and 410 nm, respectively.

4. Conclusions

Graft amphiphilic polyelectrolytes with hydrophilic main chain were shown to constitute a new class of polymeric materials that may serve as efficient stabilizers of the nanocapsules templated on liquid hydrophobic cores. Model photoactive copolymers with short grafts containing naphthalene chromophores were synthesized, characterized and applied here to enable use of a sensitive spectroscopic technique (fluorescence) to follow conformation of the macromolecules and structure of the formed capsules. While such macromolecules adopt rather compact conformation in an aqueous medium some uncoiling occurs at the water-oil interface that leads to anchoring the hydrophobic grafts in the oil phase and efficient stabilization of emulsion droplets by the charged polymer main chain. This feature makes such polymers very useful for preparation of nanocapsules with liquid hydrophobic cores that are suspended in water without a need of additional stabilizers. We reported here the formation of nanometer size capsules of spherical morphology, as showed using SEM and cryo-TEM, that were stable in aqueous emulsion over at least 2 months. We showed that morphology of such graft amphiphilic polyelectrolytes strongly affects their ability to stabilize the nanoemulsion droplets. Generally, the copolymers with higher grafting density were found to be better stabilizers of the nanocapsules. We also showed that by using LbL saturation technique stable capsules with multilayer shells may be obtained that efficiently encapsulate hydrophobic probe molecules which did not tend to aggregate in the liquid cores as they maintained their fluorescent properties. Such strategy may be easily adopted for preparation of nanocarriers of lipophilic substances, especially in the field of biomedical applications where low bioavailability of hydrophobic compounds is a limitation for their application. Such systems based on biodegradable natural polymers are currently intensively studied in our and collaborating laboratories.

Acknowledgement

The authors would like to thank the Polish Ministry of Science and Higher Education for the Financial support ("Ideas Plus" grant no. IdP2011 000561). The P2M program from the ESF is also acknowledged. J. S. acknowledges the financial support from the project Interdisciplinary PhD Studies "Molecular sciences for medicine" (co-financed by the European Social Fund within the Human Capital Operational Program).The research was carried out with the equipment purchased thanks to the financial support of the European Regional Development Fund in the framework of the Innovation Economy Operational Program (contract no. POIG.02.01.00-12-023/08).

Notes and references

[a] Jagiellonian University, Faculty of Chemistry, Ingardena 3, 30-060 Krakow, Poland. E-mail: zapotocz@chemia.uj.edu.pl

† Electronic Supplementary Information (ESI) available (spectroscopic and DLS data): See DOI: 10.1039/b000000x/

1 K. T. Kim, S. A. Meeuwissen, R. J. Nolte, J. C. van Hest, *Nanoscale*, 2010, **2,** 844.
2 J. V. Natarajan, C. Nugraha, X. W. Ng, S. Venkatraman, *J. Control. Release,* 2014, **193**, 122.
3 M. A. Trojer, H. Andersson, Y. Li, J. Borg, K. Holmberg, M. Nydén, L. Nordstierna, *Phys. Chem. Chem. Phys,* 2013, **193**, 6456.
4 M. Gonnet, L. Lethuaut, F. Boury, *J. Control. Release*, 2010, **146**, 276.
5 C.-K. Chen, O. Wang, C. H. Jones, Y. Yu, H. Zhang, W.-C. Law, C. K. Lai, Q. Zeng, P. N. Prasad, B. A. Pfeifer, C. Cheng , *Langmuir***,** 2014, **30**, 4111.
6 O. L. Johnson, W. Jaworowicz, J. L. Cleland, L. Bailey, M. Charnis, E. Duenas, C. Wu, D. Shepard, S. Magil, T. Last, A. J. Jones, S. D. Putney, *Pharm Res.*, 1997, **14**, 730.
7 M. Adamczak, H. J. Hoel, G. Gaudernack, J. Barbasz, K. Szczepanowicz, P. Warszyński, *Colloids Surf. B. Biointerfaces*, 2012, **90**, 211.
8 L. Miao, F. Liu, S. Lin, J. Hu, G. Liu, Y. Yang, Y. Tu, C. Hou, F. Li, M. Hu, H. Luo, *Langmuir,* 2014, **30**, 3996.
9 T. Bramer, M. Paulsson, K. Edwards, K. Edsman, *Pharmaceutical Res.*, 2003, **20**, 1661.
10 A. S. Narang, D. Delmarre, D. Gao, *Int. J. Pharm*., 2007, **345**, 9.
11 X.-B. Xiong, Z. Binkhathlan, O. Molavi, A. Lavasanifar, *Acta Biomater*., 2012, **8**, 2017.

12 D. Quémener, A. Deratani, S. Lecommandoux, *Topics Curr. Chem.,* 2012, **322**, 165.

13 R. Trivedi, U. B. Kompella, *Nanomedicine*, 2010, **5**, 405.

14 S. C. Owen, D. P. Y. Chan, M. S. Shoichet, 2012, *Nano Today*, **7**, 53.

15 S. De Koker, R. Hoogenboom, B. G. De Geest, *Chem. Soc. Rev.,* 2012, **41**, 2867.

16 D. Volodkin, R. von Klitzing, H. Möhwald, *Polymers*, 2014, **6**, 1502.

17 G. Decher, J. D. Hong, J. Schmitt, *Thin Solid Films*, 1992, **210,** 831.

18 D. Guzey, D. J. McClements, *Adv. Colloid Interface Sci.,* 2006, **128-130**, 227.

19 E. Donath, G. B. Sukhorukov, F. Caruso, S. A. Davis, H. Möhwald, *Angew. Chem., Int. Ed.*, 1998, **37**, 2201.

20 I. L. Radtchenko, M. Giersig, G. B. Sukhorukov, *Langmuir*, 2002, **18**, 8204.

21 G. B. Sukhorukov, E. Donath, S. Davis, H. Lichtenfeld, F. Caruso, V. I. Popov, H. Möhwald, *Polym. Adv. Technol.,* 1998, **9**, 759.

22 Y. Sun, J. Travas-Sejdic, J. Wen, R. G. Alany, *Curr. Drug Deliv.*, 2009, **6**, 332.

23 Y. Wang, F. Caruso, *Adv. Mater.*, 2006, **18,** 795.

24 T. Mauser, C. Déugnat, H. Möwald, G. B. Sukhorukov, *Langmuir,* 2006, **22***,* 5888.

25 A. V. Kabanova, H. E. Gendelman, *Prog. Polym. Sci.,* 2007, **32**, 1054.

26 K. Szczepanowicz, U. Bazyliańska, J. Pietkiewicz, L. Szyk-Warszyńska, K. A. Wilk, P. Warszyński, *Adv. Colloid. Interface Sci.,* 2014, http://dx.doi.org/10.1016/j.cis.2014.10.005

27 K. Szczepanowicz, H. J. Hoel, L. Szyk-Warszyńska, E. Bielańska, A. M. Bouzga, G. Gaudernack, C. Simin, P. Warszyński, *Langmuir,* 2010, **26**, 12592.

28 U. Bazylińska, R. Skrzela, K. Szczepanowicz, P. Warszyński, K. Wilk, *Soft Matter*, 2011, **7**, 6113.

29 U. Bazylińska, R. Skrzela, M. Piotrowski, K. Szczepanowicz, P. Warszyński, K. Wilk, *Bioelectrochemistry*, 2012, **87**, 147.

30 M. Rymarczyk-Machał, J. Szafraniec, S. Zapotoczny, M. Nowakowska, *Eur. Polym. J.***,** 2014, **55,** 76.

31 W. Xun, H.-Y. Wang, Z.-Y. Li, S.-X. Cheng, X.-Z. Zhang, R.-X. Zhuo, *Colloids Surf. B Biointerfaces,* 2011, **85**, 86.

32 K. Kita-Tokarczyk, J. Grumelard, T. Haefele, W. Meier, *Polymer*, 2005, **46**, 3540.

33 F. Liu, J. Hu, G. Liu, S. Lin, Y. Tu, C. Hou, H. Zou, Y. Yang, Y. Wu, Y. Mo, *Polym. Chem.,* 2014, **5**, 1381.

34 M. Rymarczyk-Machał, S. Zapotoczny, M. Nowakowska, *J. Polym. Sci. A Polym. Chem.,* 2006, **44**, 2675.

35 M. Nowakowska, S. Zapotoczny, A. Karewicz, *Polymer*, 2001, **42**, 1817.

36 L. W. Fischer, A. R. Sochor, J. S. Tan, *Macromolecules*, 1977, **10**, 949.

37 S. Goldstein, D. Meyerstein, *Acc. Chem. Res.,* 1999, **32**, 547.

38 S. Zapotoczny, M. Rymarczyk-Machał, A. Stradomska, P. Petelenz, M. Nowakowska, *J. Phys. Chem. B,* 2007, **111,** 10088.

39 I. Capek, *Adv. Colloid Interface Sci.*, 2002, **97**, 91.

40 M. M. Miller, S. P. Wasik, G.-L. Huang, W. Y. Siu, D. Mackay, *Environ Sci. Technol*., 1985, **19**, 522.

41 H. Evertsson, S. Nilsson, *Macromolecules*, 1997, **30**, 2377.

42 J. R. Lakowicz, *Principles of Fluorescence Spectroscopy*, Springer, New York, 3rd edn, 2006.

43 M. Nowakowska, S. Zapotoczny, A. Karewicz, *Macromolecules*, 2000, **33**, 7345.